Close-In Magnetic Fields of a Lightning Return Stroke

R. D. Jones, H. A. Watts

🔳 Sandia Laboratories

1-2

CLOSE-IN MAGNETIC FIELDS OF A LIGHTNING RETURN STROKE

R. D. Jones
EMR/EMP Analysis Division 9353

H. A. Watts
Applied Mathematics Division 2642
Sandia Laboratories
Albuquerque, NM 87115

ABSTRACT

The method of images is used to determine the time history of the close-in magnetic field environment resulting from a lightning return stroke at a point on the earth's surface and at altitudes of 2000 and 4000 meters. The lightning channel is modeled after Uman and McLain, and a Dennis and Pierce type current distribution in the channel is assumed. Particular attention is given to the initial lightning return stroke in which the velocity of stroke propagation is time varying. A constant velocity of stroke propagation is used for subsequent return strokes. Results obtained from a simplified model are compared with those obtained from a model using retarded potentials. For close-in environments, excellent agreement is obtained between the two treatments. Some observations are made about the magnetic field variation with respect to altitude and the distance of the observer from the stroke, and a versatile, easily-used computer code applicable to a wide range of lightning parameters is described.

ACKNOWLEDGEMENT

4

CLOSE-IN MAGNETIC FIELDS OF A LIGHTNING RETURN STROKE

Introduction

The possibility that the guidance system of a rocket or missile might malfunction during the boost phase of its flight as a result of exposure to the electromagnetic environment resulting from lightning is suggested by the well-documented Apollo 12 lightning incident (Brook, Holmes, and Moore, 1970). Accordingly, estimates of the time-history of the build-up of magnetic intensity resulting from a lightning return stroke should be of interest to weapon or navigation system designers concerned with the vulnerability of their systems to electromagnetic environments.

Most of the recent studies which included calculations of magnetic field intensity resulting from a lightning stroke (for example, Dennis and Pierce, 1964; Uman and McLain, 1969; Uman, 1969) emphasize the radiation, or far-field, components that would be observed at the surface of the earth. Because of the possible hazards created by lightning to aircraft or missiles in flight or to ordnance transported by aircraft in flight, this report emphasizes calculation of the magnetic field intensity at points above the surface. Fields at the surface are obtained as a special case. The particular approach used is similar to but more general than that used by Uman and McLain, 1969. In addition, the limits of integration in the expressions for the magnetic fields are treated in a different manner and a cylindrical rather than spherical geometry is used.

Although the lightning flash constitutes a very complex set of phenomena, the phenomenon of interest in this report is the magnetic field resulting from the return stroke; i.e., the second stage of a two-step process. In the first or leader stage, a few coulombs of charge are progressively removed from the thundercloud and become distributed along the whole leader channel. In the second or return stroke phase, the charge on the leader channel is transferred to ground. The phenomenon is analogous to the situation which occurs if a transmission line charged to a constant potential is short-circuited.

During the return stroke phase, the transfer of charge to the earth from progressively higher regions in the charged channel is manifested by a current surge of considerable strength. The return stroke wavefront which marks the upward progress of the current surge propagates at peak velocities which approach the speed of light. The velocity of the initial return stroke of a lightning flash varies with time, but the velocities of subsequent return strokes, typically three or four in number, tend to be constant (Uman, 1969).

On the basis of geometrical considerations, one might expect the magnetic field from a cloud-to-ground stroke at a point on the surface to be different from the magnetic field intensity in the vicinity of points above the surface. It turns out that contributions to the total field intensity from the image stroke decrease in importance with increasing altitude. However, the peak magnetic field intensity due to the initial stroke is only slightly sensitive to variations in altitude at the same radial distance from the stroke.

Although the peak field intensities from subsequent return strokes are less than those from the initial return stroke, the rise times from the former are shorter so that subsequent return strokes might cause a more severe environment. Elaborations on these aspects of the radiation phenomena and descriptions of computational techniques are given in the material which follows. The validity of certain simplifying assumptions is discussed.

Theory

Constant Return-Stroke Velocity

Following Uman and McLain (1969), the return-stroke channel is idealized as a straight line normal to a perfectly conducting plane (the earth). In order to simplify the calculation, the conducting plane can be replaced by an image line beneath the plane. The geometry is defined in Figure 1 which idealizes an upward-directed return stroke. Above the wavefront the current is assumed to be zero. Eventually, the return stroke attains its maximum height, L. The field components can be obtained from the retarded vector potential

$$\overline{A}(\rho, \varphi, \zeta, t) = \frac{\mu_o}{4\pi} \int_V \frac{1}{r} \overline{J}(z, t')dV \quad , \tag{1}$$

where μ_o is the permeability of free space; $\overline{J}$ is the current density; ρ, φ, and ζ are cylindrical coordinates of the point of observation; and t' is the retarded time, $t - r/c$, where r is the distance from the observer to a current element (see Figure 1) and c is the velocity of light.

Because the current is assumed to be entirely in the z direction, the vector potential at the observation point P has only one component, A_ζ. Upon taking into account the effect of the image current (following King, 1962) A_ζ is obtained as

$$A_\zeta(\rho, \zeta, t) = \frac{\mu_o}{4\pi} \int_0^{h(\tau)} \frac{1}{r(z)} I\left(z, t - \frac{r(z)}{c}\right) dz$$

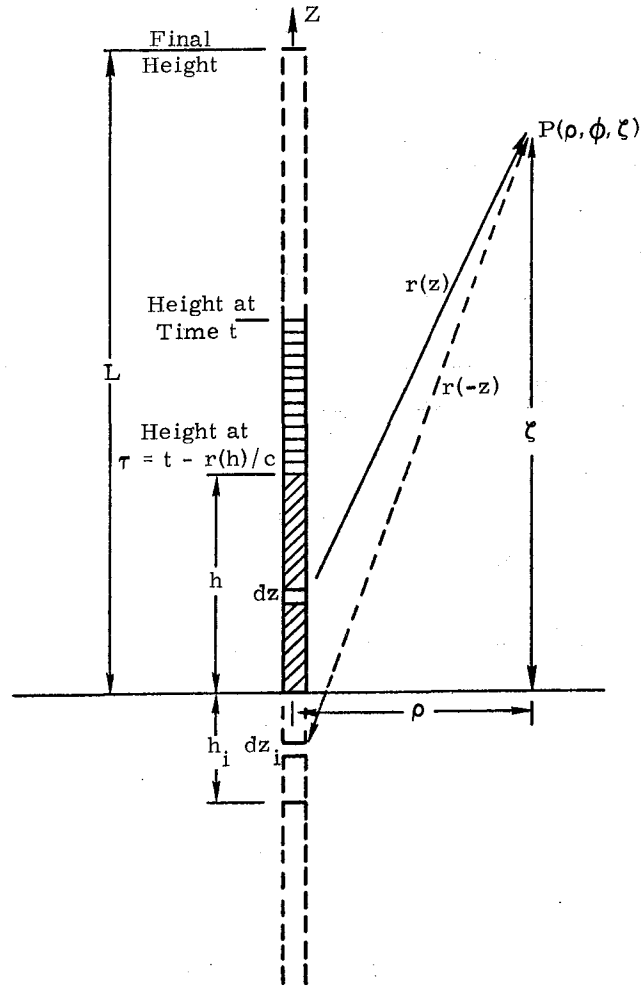$$+ \frac{\mu_o}{4\pi} \int_0^{h(\tau_i)} \frac{1}{r(-z)} I\left(z, t - \frac{r(-z)}{c}\right) dz \quad , \tag{2}$$

Figure 1. Idealization of an upward-moving return
stroke with velocity v and final height L

where

$$r(z) = \sqrt{(\zeta - z)^2 + \rho^2} \quad . \tag{3}$$

For the constant velocity model typifying subsequent return strokes, the wavefront height is defined by

$$h(t) = \begin{cases} vt, & \text{for } 0 \le t \le \tau_o , \quad \tau_o = L/v \\ L, & \text{for } t > \tau_o . \end{cases} \tag{4}$$

To avoid violation of causality, the upper limits of Eq. (2) are defined by the retarded times

$$\tau = t - \frac{r(h)}{c} = t - \frac{1}{c} \sqrt{(\zeta - h)^2 + \rho^2} \quad ,$$

$$\tau_i = t - \frac{r(-h_i)}{c} = t - \frac{1}{c} \sqrt{(\zeta + h_i)^2 + \rho^2} \tag{5}$$

(see Figure 1). For simplicity, we shall generally write h, h_i, r, and r_i in place of $h(\tau)$, $h(\tau_i)$, $r(z)$, and $r(-z)$, respectively. From Eqs. (5) and (4), one finds that

$$\tau = \frac{(c^2 t - v\zeta) - \sqrt{c^2(vt - \zeta)^2 + (c^2 - v^2)\rho^2}}{c^2 - v^2} \tag{6}$$

(meaningful only for $\tau \geq o$). A similar formula holds for τ_i except that plus signs replace the minus signs before the two ζ terms.

Using the relationship $\overline{B} = \overline{\nabla} \times \overline{A}$, the φ component of the magnetic field intensity, which is given by

$$H_\varphi = -\frac{1}{\mu_o} \frac{\partial A_\zeta}{\partial \rho} \quad , \tag{7}$$

takes the form

$$H_\varphi = \frac{-1}{4\pi} \int_o^h \frac{\partial}{\partial \rho} \left(\frac{1}{r} I(z, \ t - \frac{r}{c}) dz - \frac{1}{4\pi} \frac{\partial h}{\partial \rho} \left[\frac{1}{r} I(z, \ t - \frac{r}{c}) \right]_{z=h} \right.$$

$$-\frac{1}{4\pi} \int_o^{h_i} \frac{\partial}{\partial \rho} \left(\frac{1}{r_i} I(z, \ t - \frac{r_i}{c}) \right) dz - \frac{1}{4\pi} \frac{\partial h_i}{\partial \rho} \left[\frac{1}{r_i} I(z, \ t - \frac{r_i}{c}) \right]_{z=h_i} \tag{8}$$

The current surge of the return stroke is usually represented by

$$I(t) = I_o \left[\exp(-\alpha t) - \exp(-\beta t) \right], \quad t \geq o \tag{9}$$

a form first suggested by Bruce and Golde (1941). However, following Dennis and Pierce (1964), we assume a channel current below the return stroke wavefront of the form

$$I(z, t) = I_o \left\{ \exp\left[-\alpha \left(t - \frac{z}{v} \right) \right] - \exp\left[-\beta \left(t - \frac{z}{v} \right) \right] \right\}, \quad t \geq \frac{z}{v} \tag{10}$$

where, as before, v is the constant upward velocity of the current wave. As Dennis and Pierce (1964) point out, the advantage of Eq. (10) is that it avoids the assumption that the current is

8

uniform in the channel and instead assumes that it varies as a function of z. The disadvantage of Eq. (10) is that a constant velocity is assumed for the return stroke. This is true only for subsequent return strokes. However, the model can be adapted for the initial return stroke in which the propagation velocity changes with time. This subject is discussed in a subsequent section.

Now, if Eq. (10) is substituted in Eq. (8) it is found that the second and fourth terms on the right side of Eq. (8) vanish because of the following argument. For $\tau > \tau_o$, $h(\tau)$ is equal to L, a constant, and $\delta L/\delta\rho = 0$. During the period $0 \leq \tau \leq \tau_o$, we find that by using Eqs. (4) and (5):

$$I(z, \ t - \frac{r}{c})\bigg]_{z=h} = I(h, \ \tau) = I_o \left\{ \exp\left[-\alpha(\tau - \frac{h}{v})\right] \right.$$

$$\left. - \exp\left[-\beta(\tau - \frac{h}{v})\right] \right\} = 0 \ . \tag{11}$$

Similarly,

$$I\left(z, \ t - \frac{r_i}{c}\right)\bigg]_{z=h_i} = I(h_i, \ \tau_i) = 0 \ . $$

Then using the fact that $\dfrac{\delta r}{\delta\rho} = \rho/r$ and recognizing that

$$\frac{\delta}{\delta\rho} I\left(z, \ t - \frac{r}{c}\right) = \frac{-\rho}{cr} \frac{\delta}{\delta t} I\left(z, \ t - \frac{r}{c}\right) \ , \tag{12}$$

Eq. (8) can be written in the form

$$H_\phi(\rho, \ \zeta, \ t) = \frac{\rho}{4\pi} \int_o^h \left\{ \frac{1}{r^3} + \frac{1}{cr^2} \frac{\delta}{\delta t} \right\} I\left(z, \ t - \frac{r}{c}\right) dz$$

$$+ \frac{\rho}{4\pi} \int_o^{h_i} \left\{ \frac{1}{r_i^3} + \frac{1}{cr_i^2} \frac{\delta}{\delta t} \right\} I\left(z, \ t - \frac{r_i}{c}\right) dz \ . \tag{13}$$

The explicit form of the magnetic intensity is now obtained by substitution of Eq. (10) into Eq. (13), which results in

$$H_\phi(\rho, \ \zeta, \ t) = \frac{\rho I_o}{4\pi} \left\{ F(\alpha, \ \rho, \ \zeta, \ t) - F(\beta, \ \rho, \ \zeta, \ t) \right\} \ , \tag{14}$$

where

$$F(\eta, \rho, \zeta, t) = e^{-\eta t} \int_0^{h(\tau)} \left[\frac{1}{r^3(z)} - \frac{\eta}{cr^2(z)} \right] \exp\left[\frac{\eta z}{v} + \frac{\eta r(z)}{c} \right] dz$$

$$+ e^{-\eta t} \int_0^{h(\tau_i)} \left[\frac{1}{r^3(-z)} - \frac{\eta}{cr^2(-z)} \right] \exp\left[\frac{\eta z}{v} + \frac{\eta r(-z)}{c} \right] dz \quad . \tag{15}$$

As would be expected, if $\zeta = 0$, $h(\tau)$ and $h(\tau_i)$ are replaced by L in Eq. 13) and a transformation of coordinates is made, the expression derived by Uman and McLain (1969) for the magnetic flux density at the earth's surface is obtained. It should be noted that the essential difference in the expressions for the magnetic field intensities is that in the present derivation the observer is not limited to the surface and the magnetic environment resulting from a lightning return stroke can be calculated for missiles or aircraft in flight as the return stroke develops.

A Simplified Model

Because we are primarily interested in close-in field characteristics, assume that the influence of the retarded time is negligible. Accordingly, we shall then only be concerned with a single time variation so that the time associated with the lightning return stroke in the channel corresponds to the time associated with the observation point P. Thus, Eq. (2) becomes

$$A_\zeta(\rho, \zeta, t) = \frac{\mu_0}{4\pi} \int_0^{h(t)} \left[\frac{1}{r} + \frac{1}{r_i} \right] I(z, t) dz \quad , \tag{16}$$

where

h(t) is defined by Eq. (4) ,

and r, $I(z, t)$ are given by Eqs. (3) and (10), respectively. Because $I(h(t), t) = 0$, this is still consistent with the assumption that above the wavefront the current is assumed to be zero; that is, the current is continuous at the wavefront.

Using Eq. (7), H_φ becomes

$$H_\varphi(\rho, \zeta, t) = \frac{-1}{4\pi} \int_0^h I(z, t) \frac{\partial}{\partial \rho} \left(\frac{1}{r} + \frac{1}{r_i} \right) dz$$

$$= \frac{\rho}{4\pi} \int_0^h \left(\frac{1}{r^3} + \frac{1}{r_i^3} \right) I(z, t) dz \quad . \tag{17}$$

10

Therefore, we can express H_φ in the form of Eq. (14) where now

$$F(\eta, \rho, \zeta, t) = e^{-\eta t} \int_o^{h(t)} \left(\frac{1}{r^3(z)} + \frac{1}{r^3(-z)} \right) \exp(\eta z/v)dz \quad . \tag{18}$$

Within the ranges of distance up to 1000 meters and altitudes up to 2000 meters, we have found negligible deviation between peak values of H_φ, and almost identical late time behavior was obtained through the use of Eq. (18) as compared to the use of Eq. (15).

Variable Return-Stroke Velocity

As noted above, Eq. (10) is not appropriate for the initial return stroke because this implies that the initial velocity of the first return stroke is the maximum velocity, an unrealistic and unnecessarily restrictive assumption. Following a suggestion by Srivastava (1966), the functional form of Eq. (9) will be used to represent the return stroke velocity. Therefore, let

$$v(t) = v_o \left(e^{-\gamma t} - e^{-\delta t} \right) , \quad t \geq 0 \quad . \tag{19}$$

It should be noted that for very large values of δ, Eq. (19) approaches the expression suggested by Bruce and Golde (1941) for the velocity of the first return stroke, that is,

$$v(t) \approx v_o e^{-\gamma t} \quad . \tag{20}$$

The channel height h now becomes

$$h(t) = v_o \left\{ \frac{1 - e^{-\gamma t}}{\gamma} - \frac{1 - e^{-\delta t}}{\delta} \right\} , \tag{21}$$

and the maximum channel length is

$$L = v_o \left(\frac{1}{\gamma} - \frac{1}{\delta} \right) \quad . \tag{22}$$

Next, it is necessary to extend the definition of $I(z, t)$ as given by Eq. (10) while still maintaining continuity of the current at the wavefront. This can be done by observing that (z/v) in Eq. (10) represents a time variable, say t_z, which depends on z and satisfies the condition $0 \leq t_z \leq t$, where $t = t_{h(t)}$. A natural extension of Eq. (10) in terms of a variable velocity $v(t)$ is given by

$$I(z, t) = I_o \left\{ \exp \left[-\alpha(t - t_z) \right] - \exp \left[-\beta(t - t_z) \right] \right\} , \tag{23}$$

where t_z is uniquely determined from Eq. (21) by taking $z = h(t_z)$ for any given z satisfying the condition $0 \le z \le h(t) \le L$. Therefore, $t_z = h^{-1}(z)$ and it is easily seen that $t_{h(t)} = h^{-1}\left[h(t)\right] = t$, thereby satisfying the requirement that the current must be continuous at the wavefront. Although t_z cannot be expressed in a simple form, the solution of $z = h(t_z)$ is well defined and presents no computational difficulties (h increases monotonically). We simply use a Newton iteration scheme. It should be noted that if γ is zero and δ is infinite, $h(t) = vt$ and Eq. (23) reduces to Eq. (10).

If we now use Eq. (23) instead of Eq. (10) in the simplified model (Eq. (16)), we obtain reasonably accurate estimates of the initial stroke close-in environment. Expressing these results in the form of H_ϕ given by Eq. (14), we see that

$$F(\eta, \rho, \zeta, t) = e^{-\eta t} \int_0^{h(t)} \left[\frac{1}{r^3(z)} + \frac{1}{r^3(-z)}\right] \exp(\eta t_z)dz \quad , \tag{24}$$

where the upper limit, h(t), is defined by Eq. (21).

Varying Velocity in Retarded Time Model

We shall now examine the implementation of the variable return-stroke velocity in the model which takes into account retardation effects. We, of course, use the more general definitions of v(t), h(t), and I(z, t) as defined by Eqs. (19), (21), and (23), respectively. The parameter t_z is again computed (by means of a Newton iteration scheme) as the solution of

$$h(t_z) = z \quad , \tag{25}$$

for given z.

The retarded time τ and the wavefront height $h(\tau)$ are once again defined as the solutions of a coupled pair of equations. Unfortunately, this time we are not able to resolve them algebraically. The equations to be solved are

$$\tau = t - \frac{r(h(\tau))}{c} = t - \frac{1}{c} \sqrt{(\zeta - h(\tau))^2 + \rho^2}$$

and

$$h(\tau) = v_0 \left\{\frac{1 - e^{-\gamma \tau}}{\gamma} - \frac{1 - e^{-\delta \tau}}{\delta}\right\} \tag{26}$$

for given t, c, ζ, ρ, v_0, γ, and δ. Since the first equation resolves τ in terms of h, we merely substitute the first formula into the second and use a Newton iteration scheme on the single equation to solve for $h(\tau)$. Clearly, we could have reversed the process to solve for τ first, but, in

any case, the solution procedure is well defined and causes no computational difficulties. In the same way we also obtain the corresponding image wavefront height $h(\tau_i)$, using the definition of τ_i from Eq. (5).

Having obtained $h(\tau)$ and $h(\tau_i)$, the explicit form of the magnetic intensity is, repeating Eq. (14),

$$H_\phi(\rho, \zeta, t) = \frac{\rho I_o}{4\pi} \left\{ F(\alpha, \rho, \zeta, t) - F(\beta, \rho, \zeta, t) \right\} , \qquad (27)$$

where now

$$F(\eta, \rho, \zeta, t) = e^{-\eta t} \int_0^{h(\tau)} \left[\frac{1}{r^3(z)} - \frac{\eta}{cr^2(z)} \right] \exp\left[\eta t_z + \eta \frac{r(z)}{c} \right] dz$$

$$+ e^{-\eta t} \int_0^{h(\tau_i)} \left[\frac{1}{r^3(-z)} - \frac{\eta}{cr^2(-z)} \right] \exp\left[\eta t_z + \eta \frac{r(-z)}{c} \right] dz . \qquad (28)$$

We wish to point out that the constant velocity model can be simulated using this formulation by merely setting $\gamma = 0$, $\delta = \infty$ and appropriately defining $h(t)$. Furthermore, by choosing $c = \infty$ we can also simulate the simplified model. Hence, the latter construction represents a completely general formulation so that we need only one basic computational algorithm to examine the various models discussed in this paper.

Choice of Parametric Values -- By setting v_o equal to the speed of light and taking γ and δ to be 4×10^4 sec^{-1} and 9×10^4 sec^{-1}, respectively, the channel length between ground and the thundercloud charge center is calculated from Eq. (22) to be roughly 4 km. This length was suggested by Dennis and Pierce (1964) and is close to the representative length of 5 km given by Uman (1969). From Eq. (19), the maximum velocity of the initial return stroke is found to be 8.7×10^7 $msec^{-1}$. This velocity is attained approximately 16 microseconds after initiation of the return stroke. A nominal propagation velocity of 8×10^7 $msec^{-1}$ is typical of subsequent return strokes (Uman, 1969).

Most authorities agree on typical values for the other three parameters associated with the return stroke current. Following Cianos and Pierce (1972), the following values were used: $\alpha = 1.7 \times 10^4$ sec^{-1} and $\beta = 3.5 \times 10^6$ sec^{-1}. The peak current in the channel was taken to be 20 kA. Other parameters of interest for present purposes are given in Table I.

TABLE I

Range of Values for Lightning Parameters
(After Cianos and Pierce, 1972)

| Parameter	Minimum	Typical	Maximum
Number of return strokes per flash	1	2 to 4	26
Duration of flash (s)	0.03	0.2	2
Time between strokes (ms)	3	40 to 60	100
Peak current per return stroke (kA)	1	10 to 20	250
Charge per flash (C)	1	15 to 20	400
Time to peak current (μs)	< 0.5	1.5 to 2	30
Rate of rise (kA/μs)	< 1	20	210
Time to half-value (μs)	10	40 to 50	250
Duration of continuing current (ms)	50	150	500
Peak continuing current (A)	30	150	1600
Charge in continuing current (C)	3	25	330

Discussion

Codes were written for the CDC (Control Data Corporation) Model 6600 computer to evaluate the four models described above. Plots of magnetic field intensity given by Eqs. (14), (24), and (28) were generated by a Stromberg Datagraphics Corporation Model 4460 plotter. Numerous computations which were performed indicate that the simplified model is adequate for determining close-in magnetic fields. The results are summarized here, and some representative plots are shown.

The order of presentation will follow the text discussion. First, we consider the magnetic field intensity from a subsequent return stroke (constant stroke propagation velocity model, Eq. (14)). Particular emphasis is placed on the contribution of the image stroke to the total field and how the importance of this contribution decreases as the height of the observer increases. Next, we consider the modification produced on the magnetic field intensity if the effects of retardation are neglected (simple model, Eq. (24)). Then, the magnetic field intensities resulting from the initial return stroke (variable stroke propagation velocity model, Eq. (28)) are described and compared with field intensity calculations based on the simple model. Finally, the magnetic field intensities resulting from the initial and subsequent return strokes are compared. Both models are used.

The solid curve in Figure 2 shows the magnetic field at the surface obtained by the superposition of the fields due to the actual return stroke and its image. The image field is indicated by the plot symbol x. Obscured by the x's are dots which represent the field resulting from the return stroke. The total magnetic field intensity is simply twice the image field.
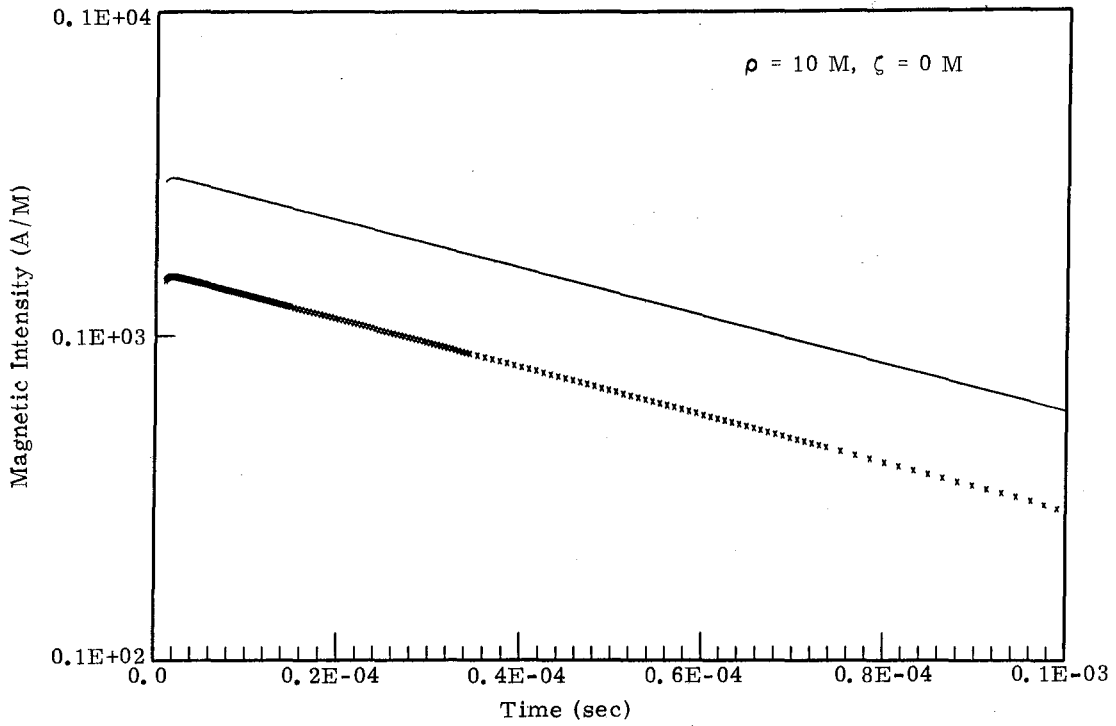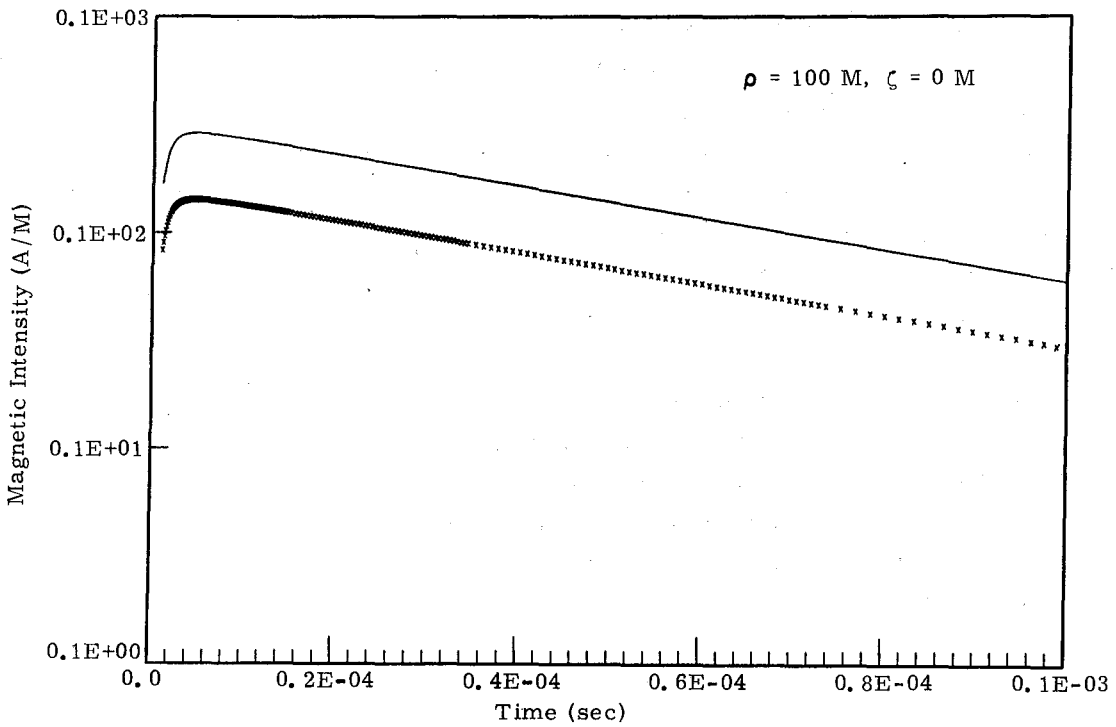
Figure 2. Magnetic field intensity versus time resulting from a subsequent
return stroke of 20 kA (Retarded Model). Data points represent
contributions of the image stroke to the total field.

The effects of retardation in Figure 2 are more pronounced than in Figure 3 which shows that the contribution from the image stroke to the total magnetic field intensity is negligible. At 2000 meters elevation most of the magnetic field is produced by the direct stroke (dots). Also, the effect of increased radial distance on the rise time is quite marked and the peak field intensity appears to vary simply inversely with radial distance at comparable altitudes. Numerous computations indicate the validity of a simple scaling relationship. If $H_\phi(\rho_o, \zeta, t)$ represents some reference field intensity where $0 < \rho_o \leq 1000$ m, then H_ϕ can be approximated by

$$H_\phi(\rho, \zeta, t) \approx \left[\frac{\rho_o}{\rho}\right] H_\phi(\rho_o, \zeta, t) \quad . \tag{29}$$

Indeed, for small values of ρ_o and ρ (e.g., on the order of 100 m or less) or when ρ is reasonably close to ρ_o, the error resulting from the use of Eq. (29) is less than 10 percent. On the other hand, if ρ_o and ρ are not close to the same value (for example, let ρ_o and ρ be 1 m and 1000 m, respectively), use of Eq. (29) could result in an over-estimate of H_ϕ of from 25 to 50 percent for the specific values cited.

Calculated absolute peak field intensities for representative values of ρ and ζ using the assumed values of the parameters I_o, α, β, v_o, γ, and δ described above are given in Table II.

Figure 4 shows that above the surface the effects of the direct stroke are still dominant although the contribution to the total field from the image stroke might be significant at early times. Referring now to the bottom graph of Figure 4, the pronounced discontinuity in the image field at 78 microseconds is a consequence of the assumption of a constant return stroke velocity. The propagation of the stroke stops abruptly when the stroke reaches a height of 4 km, resulting in a discontinuity also in the direct field component which occurs earlier in time, roughly at 53 microseconds. Also clearly evident in Figure 4 is the degradation in rise time of the magnetic field intensity with distance between the observer and the lightning return stroke.

Figure 5 shows a comparison between the results obtained using Eqs. (15) and (18) to compute the field intensity assuming a constant stroke propagation velocity (subsequent return stroke). Evidently, the effects of retardation are insignificant if the observer is close to the return stroke. The effects of retardation are only slightly more obvious in Figure 6 which compares the results obtained using Eqs. (24) and (28) to compute field intensities assuming a variable stroke propagation velocity (initial return stroke).
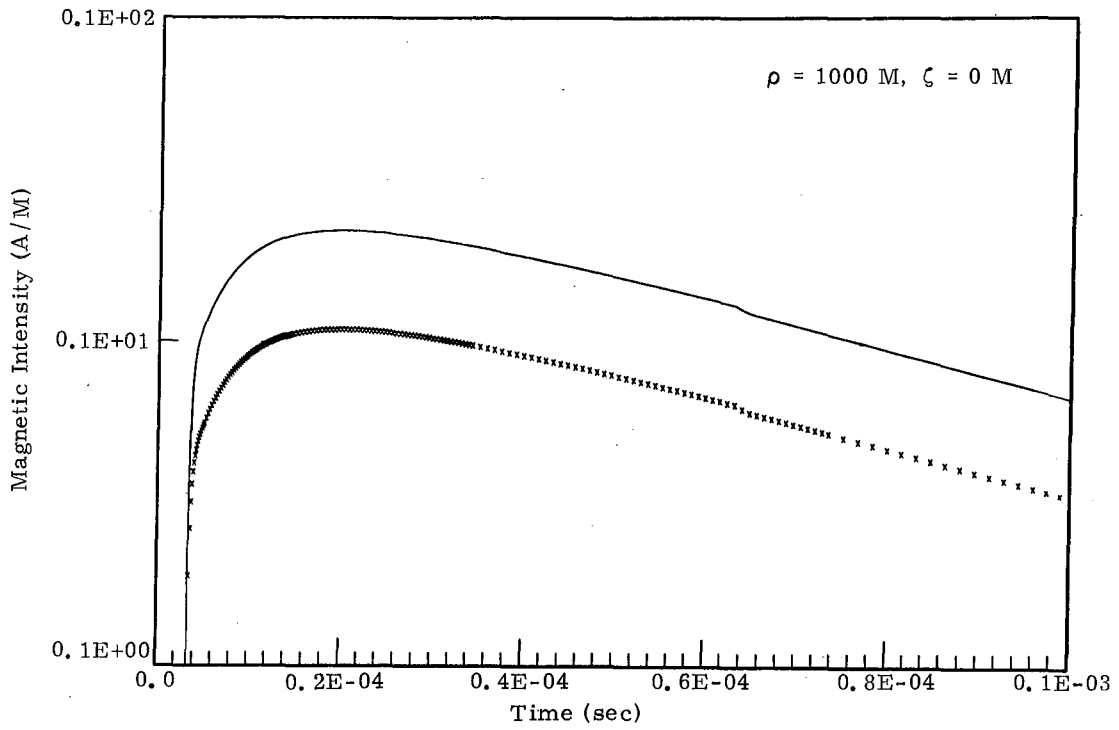
16
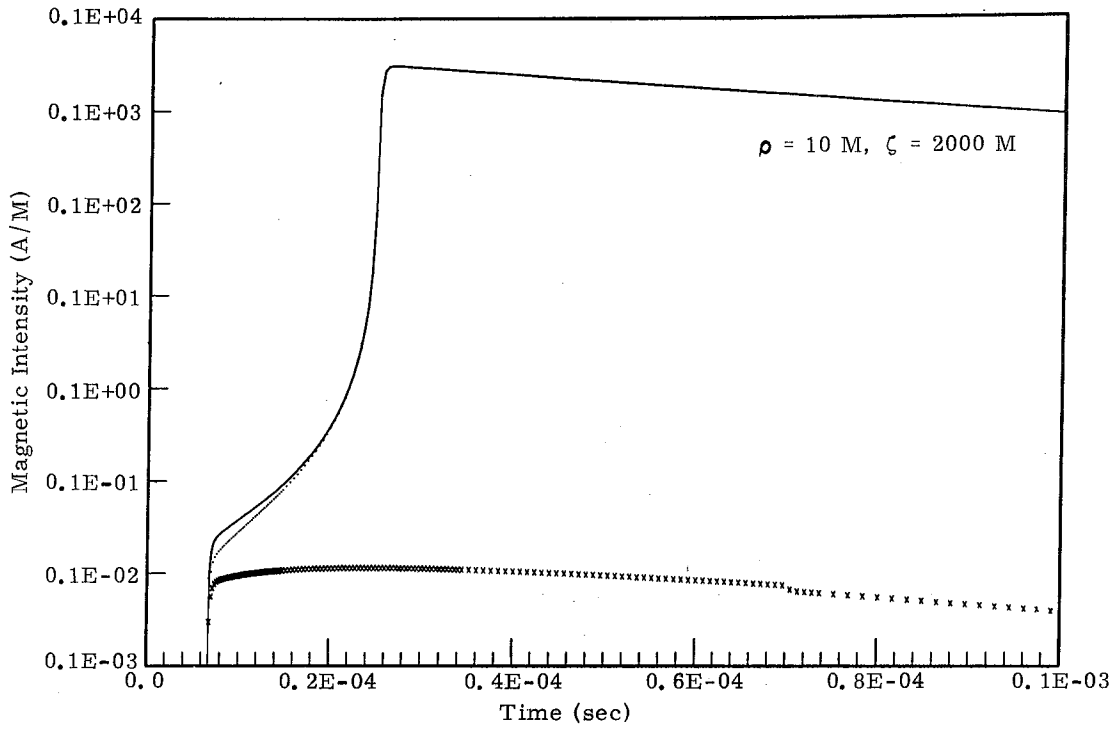
(a)
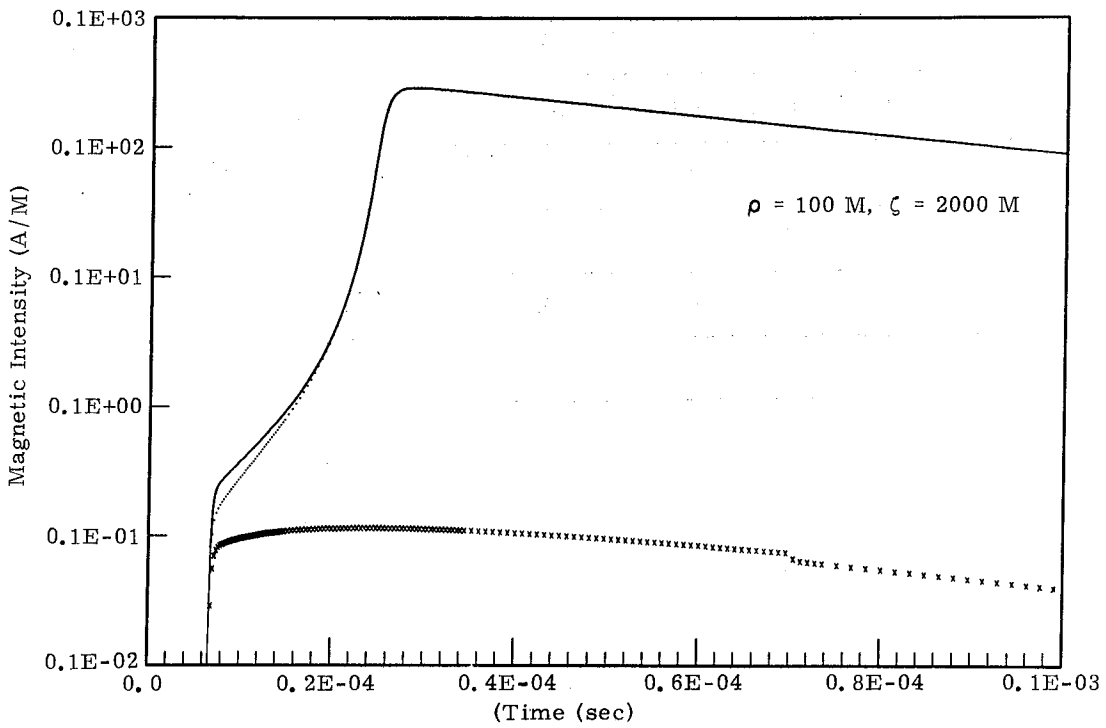
(b)

Figure 3. Magnetic field intensity versus time resulting from a subsequent
return stroke of 20 kA. (Retarded Model) Dots and crosses repre-
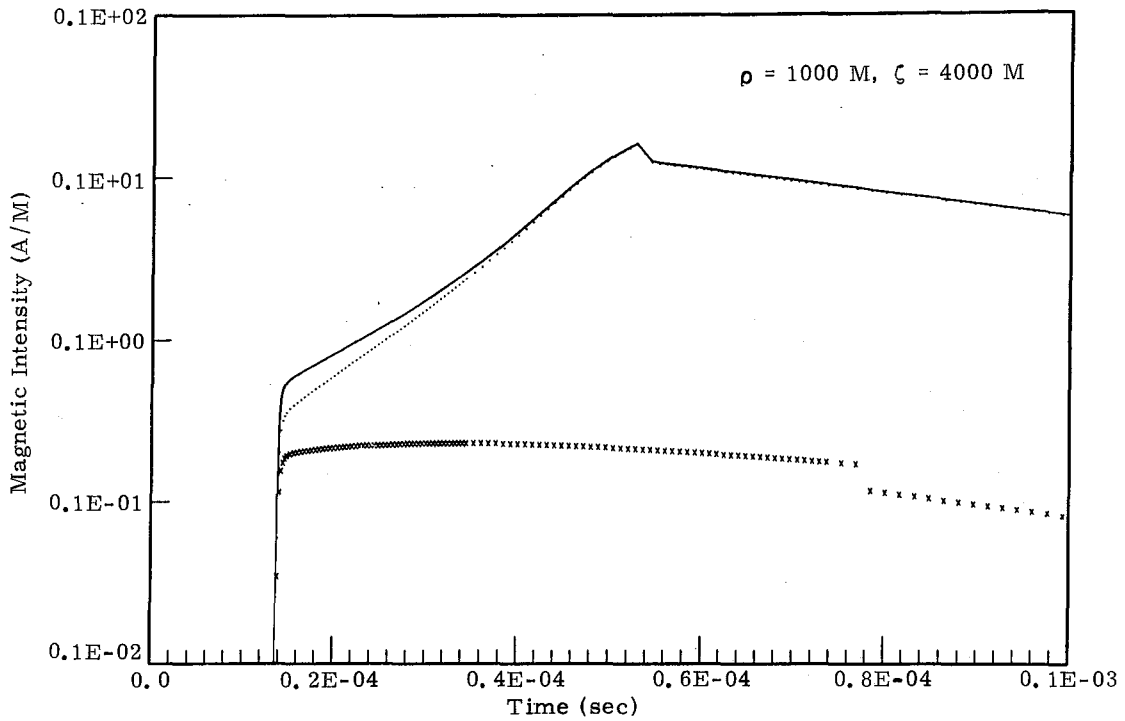sent contributions of direct and image return strokes, respectively.

TABLE II

Peak magnetic field intensities (A/meter) for representative
radial distances ρ and altitude ζ resulting from a typical
initial return stroke

(Simplified-model, variable velocity)

| ζ / ρ	0	1000	2000	3000	4000
1	3078	3085	3072	3052	3053
10	301	307	307	304	282
100	28	29	29	27	19
500	4.9	4.9	4.7	4.1	2.1
1000	2.2	2.1	2.0	1.6	0.88

Figure 4. Magnetic field intensity versus time resulting from a subsequent return stroke of 20 kA. (Retarded Model). Dots and crosses represent contributions of direct and image return strokes, respectively. Discontinuities indicate times at which observer notes end of propagation of the direct and image strokes, respectively.
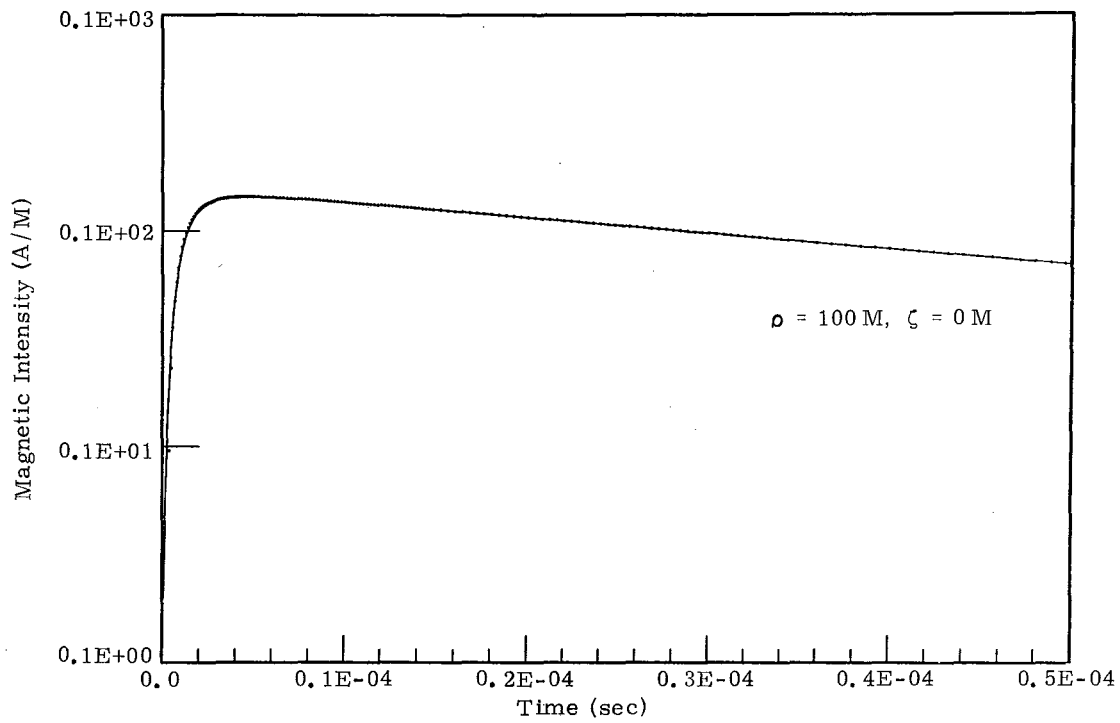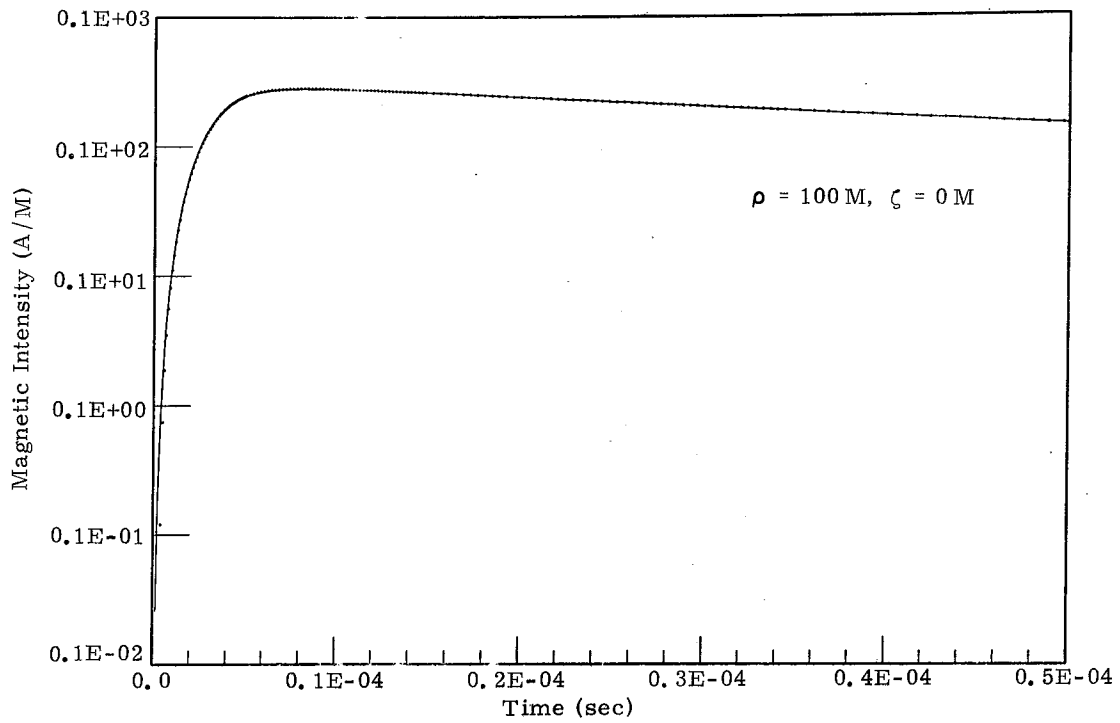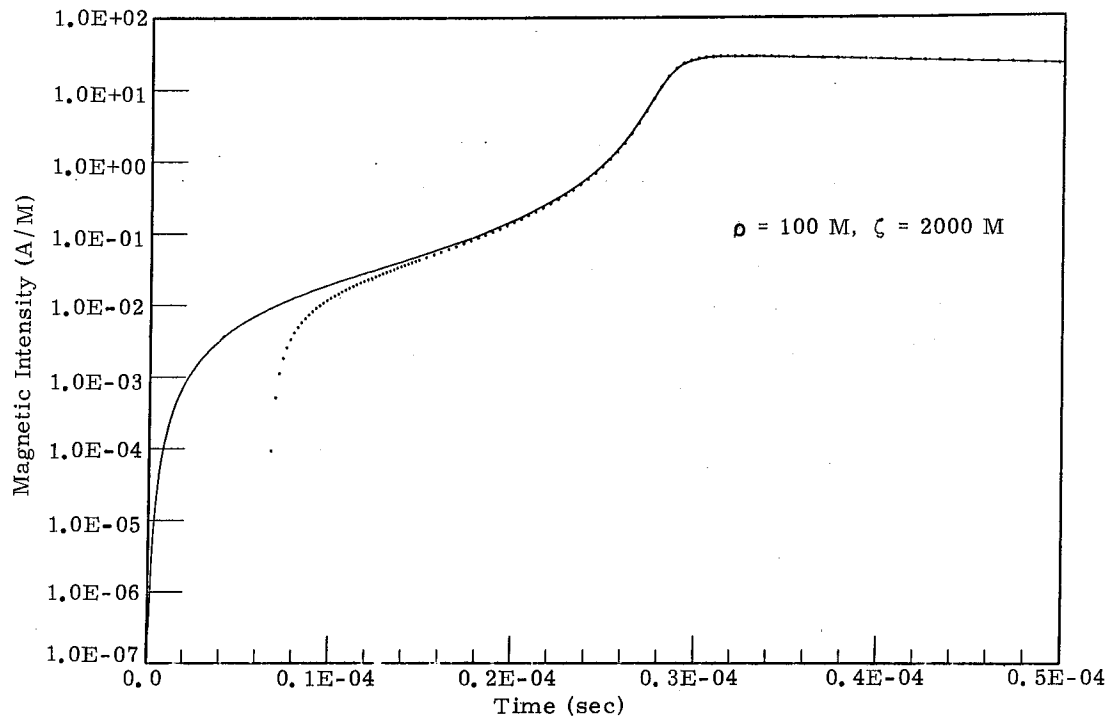
(a)
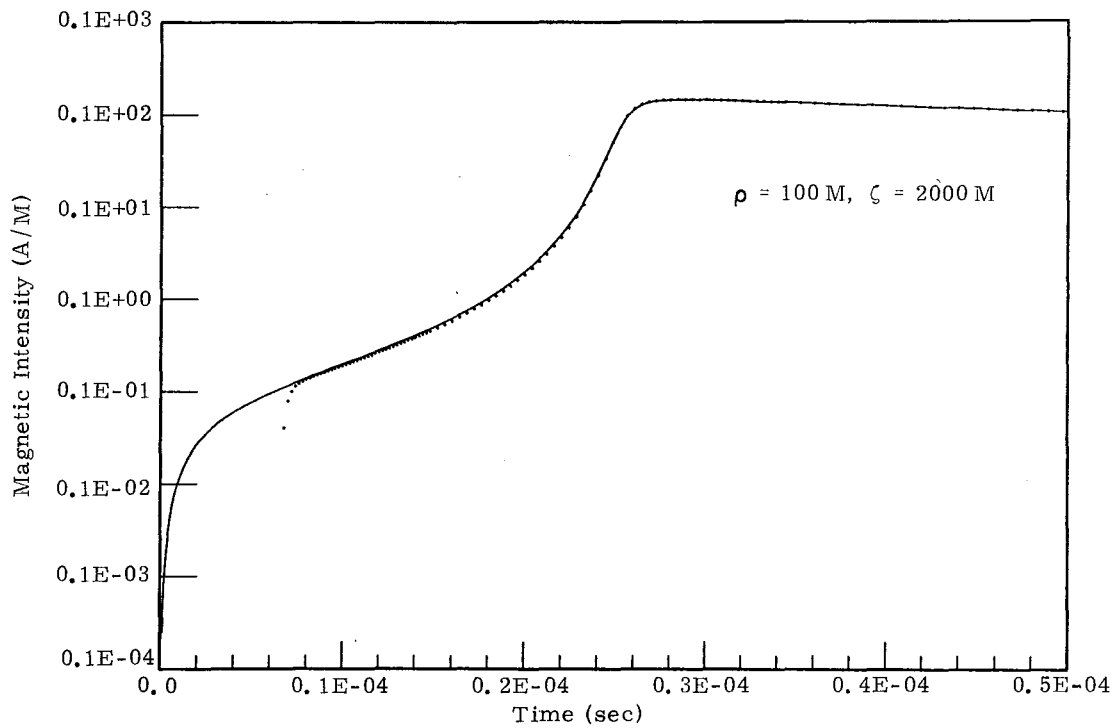
(b)

Figure 5. Magnetic field intensity versus time resulting from a 10 kA
subsequent return stroke. Note comparison between the
simple model (solid curve) and retarded model (dots)

Figure 6. Magnetic field intensity versus time resulting from a 20 kA
initial return stroke. Note comparison between the simple
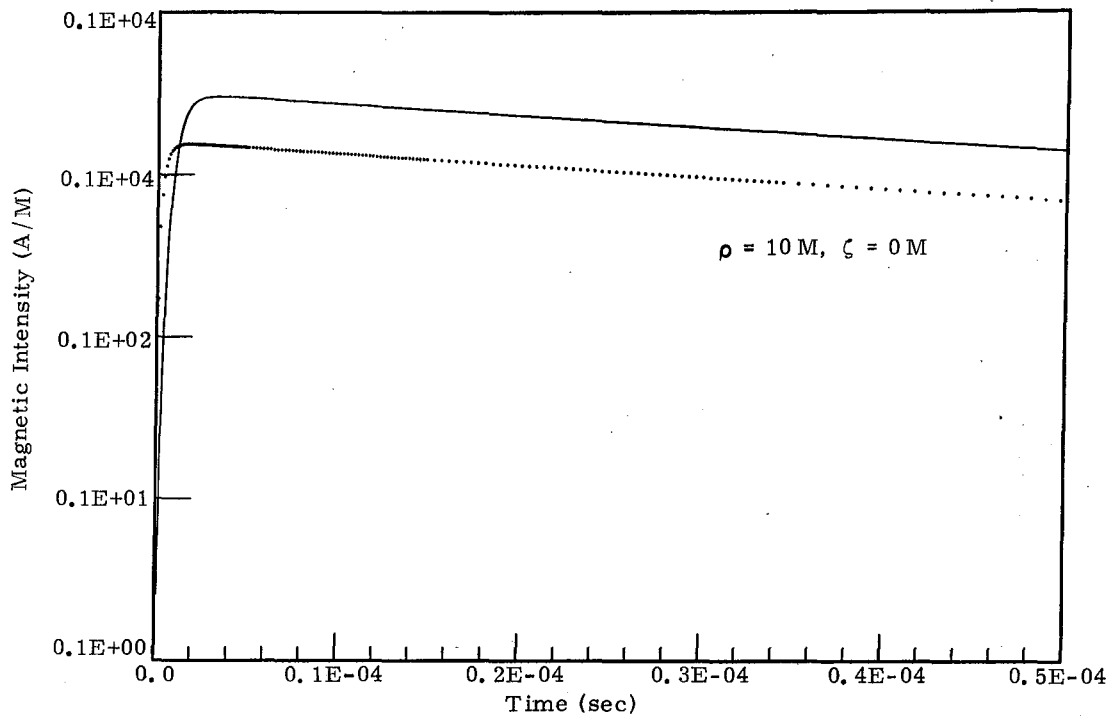model (solid curve) and retarded model (dots).

Figures 7, 8, and 9 show the magnetic field intensities associated with a typical lightning flash (see Table I). In each figure, results using the simple models are compared with the results obtained when the effects of retardation are included. That the effects of retardation can significantly modify the early time wave form is indicated in Figure 9, but peak amplitudes are little affected. Calculated absolute peak field intensities assuming a constant return stroke propagation velocity are given in Table III. Values of ρ, ζ, I_o, α, and β used in the computations for Table III are the same as those used in the computations for Table II. Comparison of Tables II and III shows that the peak field intensities of corresponding locations are almost equal except at an altitude of 4000 m. The discrepancy apparently is the result of the abrupt stop of the stroke propagation caused by assuming a constant velocity. At ζ = 4000 m, the observer is closer to the terminal point of the stroke.

A comparison of each of Figures 7, 8, and 9 shows that although the peak field intensity of the subsequent return stroke is 6 dB lower than the initial return stroke, the rise-time of the former is less than that of the latter. Therefore, fields associated with subsequent return strokes may constitute a more severe environment.
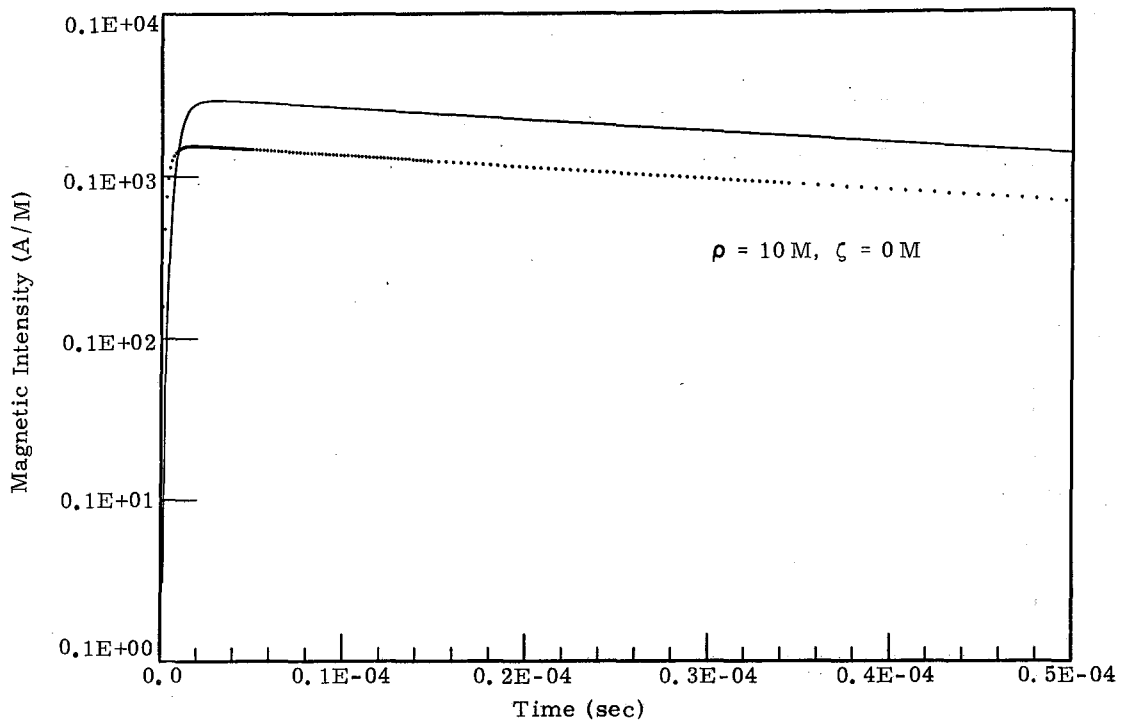
For the convenience of anyone interested in the hazards associated with a specific set of parametric values, the code used to calculate the magnetic field intensities resulting from lightning return strokes is available on tape. Retardation effects are taken into account in the computation which uses Eqs. (3), (5), (21), (26), (27), and (28). Detailed instructions on the use of this code are given in Appendix A.

All calculations show that the late time (times greater than 100 microseconds) nature of the radiation from a return stroke can be approximated very well by the Biot-Savart relationship if the current is expressed as I_o exp $(-\alpha t)$. One e-folding time for an alpha of 1.7×10^4 is roughly 60 microseconds. The magnetic fields decay so rapidly that the superposition of the magnetic fields from several return strokes would have negligible effect on the composite field. A typical flash may consist of from 3 to 4 strokes, with a time interval between strokes of 40 msec (Uman, 1969). (See also Table I.) The implication here is that deleterious effects on any complex electronic system resulting from the magnetic field environment caused by a lightning stroke must be evaluated on the basis of the threat imposed by each stroke of a multistroke flash.

Finally, it should be noted that the peak field intensity is directly proportional to the magnitude of the return stroke current, which might in a very few cases be an order of magnitude larger than the nominal 20 kA value used in this study. Because skin depth varies inversely as the square root of frequency, lightning can induce a substantial low-frequency magnetic field inside even a well shielded enclosure. This should concern designers of any systems using magnetic sensing or storage devices, for example guidance, navigation, or the dispatch of energy, fuel, or personnel.
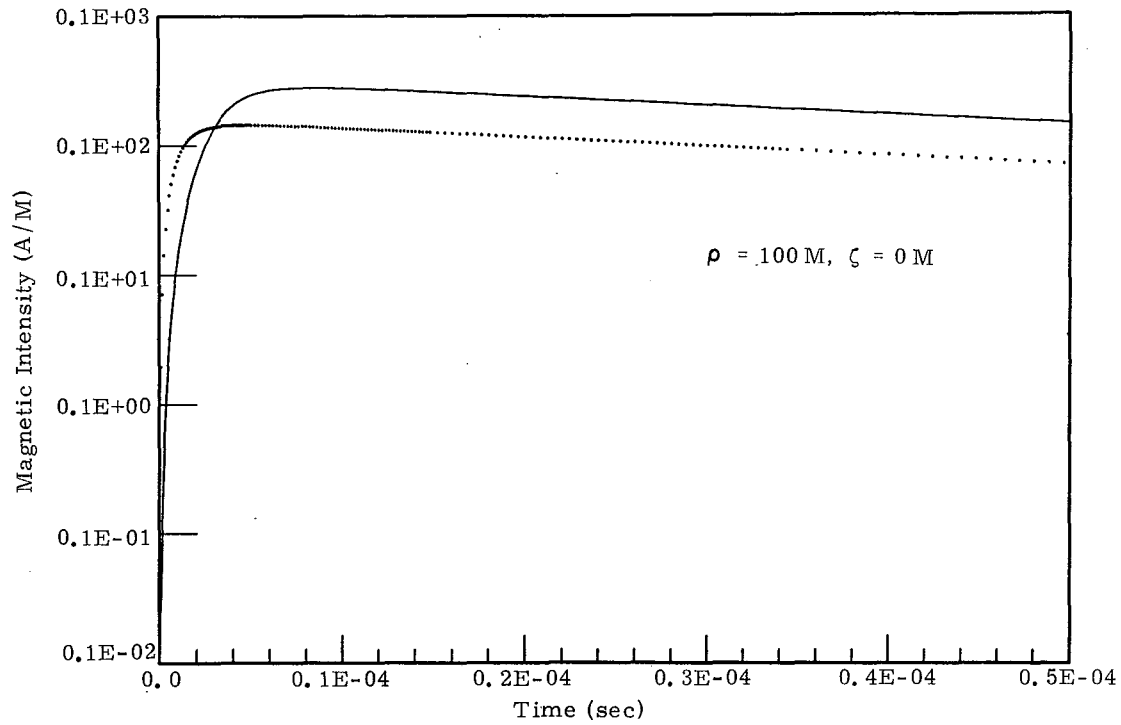
0.1E+04

0.1E+04

Magnetic Intensity (A/M)

0.1E+02

ρ = 10 M, ζ = 0 M

0.1E+01

0.1E+00

0. 0   0. 1E-04   0. 2E-04   0. 3E-04   0. 4E-04   0. 5E-04

Time (sec)

(a)

0.1E+04

0.1E+03

Magnetic Intensity (A/M)

ρ = 10 M, ζ = 0 M

0.1E+02

0.1E+01

0.1E+00

0. 0   0. 1E-04   0. 2E-04   0. 3E-04   0. 4E-04   0. 5E-04
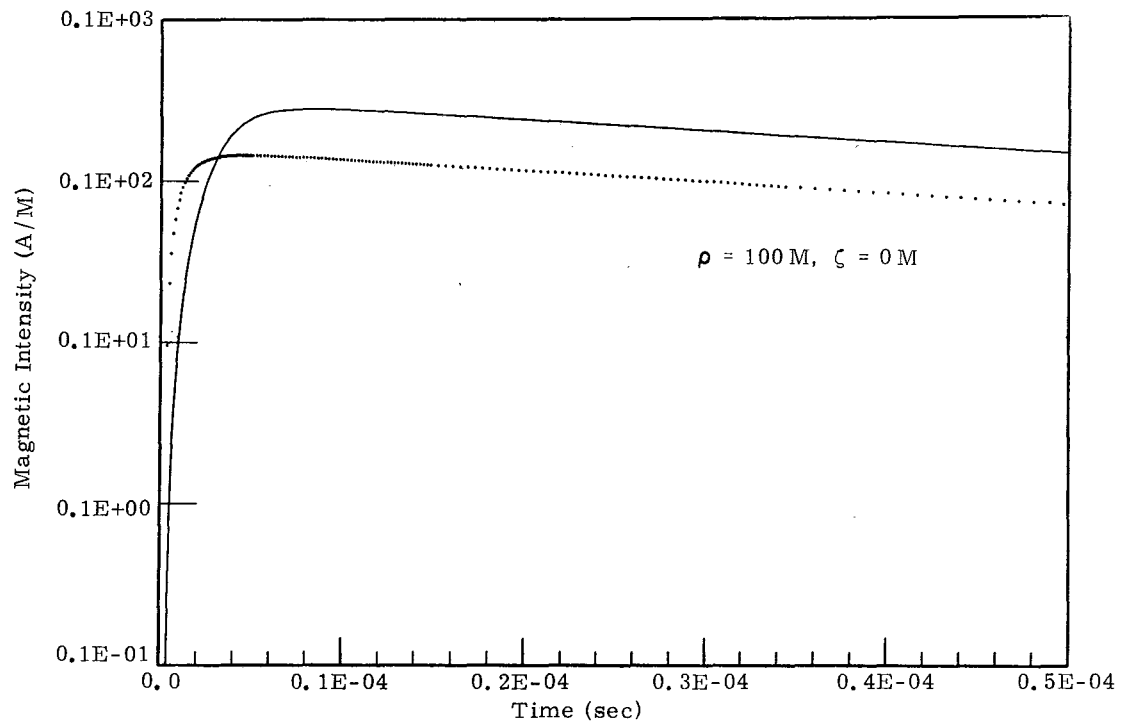
Time (sec)

(b)

Figure 7. Magnetic field intensity versus time for a nominal 20 kA initial return
stroke (solid) and a 10kA subsequent return stroke (dotted). Top figure
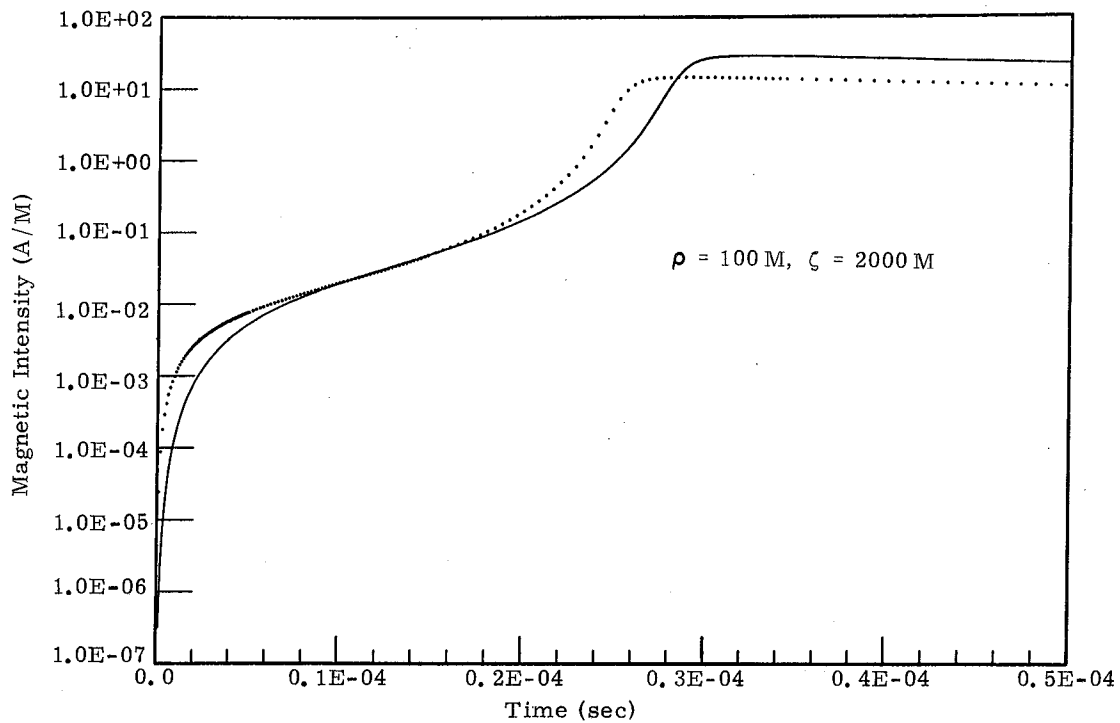is simple model, bottom figure includes retardation effects.

0.1E+03

0.1E+02

Magnetic Intensity (A/M)

0.1E+01

0.1E+00

0.1E-01

0.1E-02

0. 0   0. 1E-04   0. 2E-04   0. 3E-04   0. 4E-04   0. 5E-04

Time (sec)

ρ = 100 M, ζ = 0 M

(a)

0.1E+03

0.1E+02

Magnetic Intensity (A/M)

0.1E+01

0.1E+00

0.1E-01

0. 0   0. 1E-04   0. 2E-04   0. 3E-04   0. 4E-04   0. 5E-04
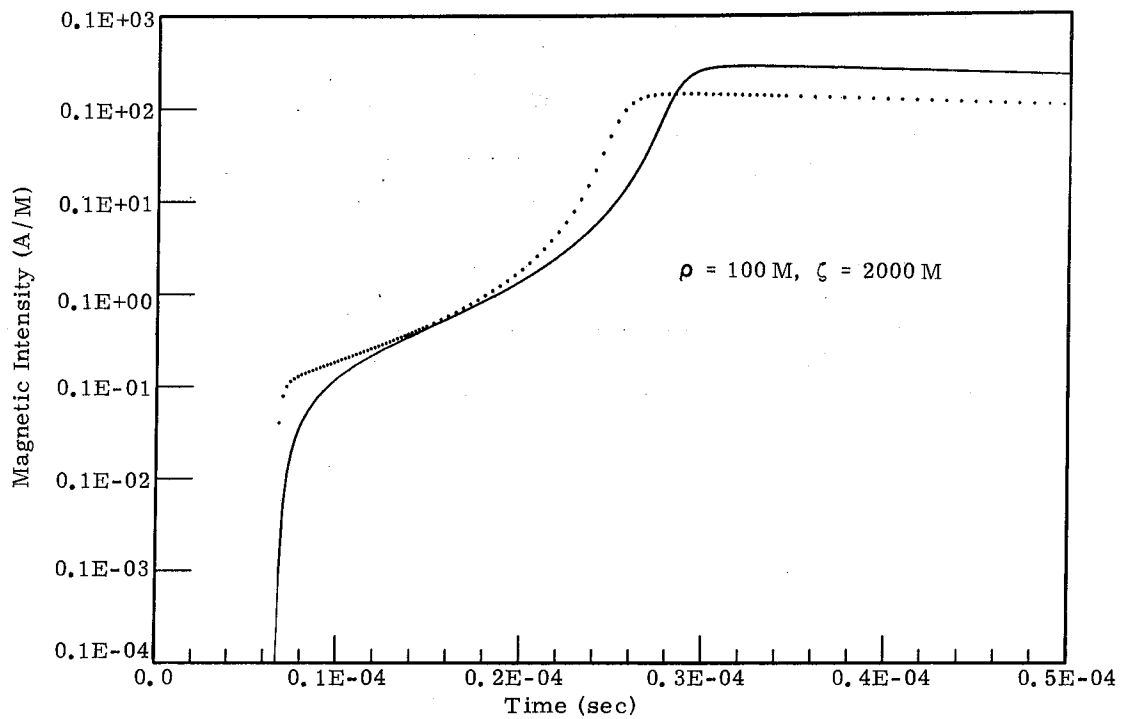
Time (sec)

ρ = 100 M, ζ = 0 M

(b)

Figure 8. Magnetic field intensity versus time for a nominal 20 kA initial re-
turn stroke (solid) and a 10 kA subsequent return stroke (dotted). Top
figure is simple model, bottom figure includes retardation effects.

24

Figure 9. Magnetic field intensity versus time for a nominal 20 kA initial return stroke (solid) and a 10 kA subsequent return stroke (dotted). Top figure is simple model, bottom figure includes retardation effects.

TABLE III

Peak magnetic field intensities (A/meter) for representative
radial distance ρ and altitude ζ resulting from a
subsequent return stroke (I_O = 20 kA)

(Retardation corrections, constant velocity)

ρ \ ζ	0	1000	2000	3000	4000
1	3086	3084	3074	3060	1522
10	307	307	307	306	153
100	29	29	29	29	15
500	4.9	4.9	4.9	4.9	3.2
1000	2.2	2.2	2.1	2.1	1.6

References

1. M. Brook, C. R. Holmes and C. B. Moore, 1970: "Lightning and Rockets: Some Implications of the Apollo 12 Lightning Event," Naval Res. Rev., 23, 1-7.

2. C. E. R. Bruce and R. H. Golde, 1941: "The Lightning Discharge," J. IEE, 88 (Pt. 2), 487-524.

3. N. Cianos and E. T. Pierce, 1972: A Ground-Lightning Environment for Engineering Usage, Stanford, Stanford Research Institute Report, SRI Project 1834, 54.

4. A. S. Dennis and E. T. Pierce, 1964: "The Return Stroke of a Lightning Flash to Earth as a Source of VHF Atmospherics," Radio Sci., 68D, 777-794.

5. K. M. L. Srivastava, 1966: "Return Stroke Velocity of a Lightning Discharge," J. Geophys Res., 71, 1283-1286

6. M. A. Uman, 1969: Lightning, New York, McGraw-Hill Book Co., 4.

7. M. A. Uman and D. K. McLain, 1969: "Magnetic Field of Lightning Return Stroke," J. Geophys. Res., 74, 6899-6970.

8. Ronald W. P. King, 1962: Fundamental Electromagnetic Theory, New York, Dover Book Co., 305-311.

APPENDIX A

An executable program on magnetic tape for the CDC 6600 computer is available for the computation of the magnetic environment resulting from cloud-to-ground lightning strokes. This appendix describes the execution of this program. The control stream required follows:

```
JØBCARD, MTI.
ACCØUNT, S123456789,A1234567,D1234,G1234,RP,KUNC.
LABEL,FILE1,R,L=FULMIN-HFIELD,VSN=19956,PW=RDJHAW.  VSN=19956
UPDATE,P=FILE1,F.
FTN,I=CØMPILE,L=0.
CØLLECT,LGØ,FXMATH,FTNLIB.
PRESET,PIND.
LGØ.
(7/8/9)
    (DATA CARDS - 6 REQUIRED)
(7/8/9)
(6/7/8/9)
```

Six data cards are required. The order of the cards, the required format, and an explanation of the parameters are given in Table A-I. The first five parameters define the starting and ending time with respect to the observer. It should be noted that the time increment can be modified in order to emphasize those times during which the field intensity is changing most rapidly.

As the program executes, the nongeometrical parameters are listed first and then the computed field intensities are printed out in tabular form preceded by the coordinates of the observer. Table A-II shows a typical output, in fact, the output plotted in Figure 2. The first column lists time with respect to stroke initiation, and the second and third columns show the retarded heights of the direct and image strokes, respectively. The fourth and fifth columns give the contributions to the composite field intensity (sixth column) from the direct and image strokes, respectively.

Again referring to Table A-I, it should be noted that reference is made to a file called Tape 11. As print out occurs, the time, direct, image, and composite field intensities, respectively, are written in Tape 11. This file can be used to transfer un-edited data between memory and either magnetic tape units or disk files. The preamble (first entry) in the file contains, respectively, the radial distance of the observer from the stroke, the height of the observer above the ground plane, and two dummy constants having the value 2.2222E+22. After all computations associated with a given set of parameters have been completed, an end-of-file is written and the computations

TABLE A-I

```
      PROGRAM LIGHT(INPUT,OUTPUT,TAPE11)
C
C     PROGRAM LIGHT COMPUTES MAGNETIC FIELD INTENSITY RESULTING FROM A
C     LIGHTNING RETURN STROKE INCLUDING THE EFFECTS OF RETARDATION.
C
C     INPUT PARAMETERS FOLLOW
C
C     NT = NUMBER OF TIME STEPS BEFORE INCREMENT IS CHANGED
C     DT = INITIAL TIME INCREMENT
C     KTI = FACTOR DEFINING INITIAL STARTING TIME KTI*DT
C     DTF = FACTOR BY WHICH TIME INCREMENT IS MODIFIED EVERY NT STEPS
C     TF = FINAL TIME
C     HH = STROKE HEIGHT (M)
C     VO = STROKE PROPAGATION VELOCITY
C     ALP,BET = BRUCE-GOLDE PARAMETERS
C     XIO = PEAK RETURN STROKE CURRENT
C     GAM,DEL = SRIVASTAVA PARAMETERS (VARIABLE STROKE VELOCITY)
C     NRHO = NUMBER OF RADIAL DISTANCES TO BE COMPUTED
C     RHO = RADIAL DISTANCE OF OBSERVER FROM STROKE (M)
C     NZP  = NUMBER OF ALTITUDES TO BE COMPUTED
C     ZP = ALTITUDE OF OBSERVER ABOVE GROUND PLANE (M)
C     FOR CONSTANT VELOCITY MODEL SET GAM=0.
C
      READ 10,NT,KTI,DTF,DT,TF,HH,VO,ALP,BET,XIO
      READ 30,GAM,DEL
      READ 20,NRHO
      READ 30,(RHO(I),I=1,NRHO)
      READ 20,NZP
      READ 30,(ZP(I),I=1,NZP)
C
   10 FORMAT (I5,I5,2F5.0,6F10.0)
   20 FORMAT(16I5)
   30 FORMAT(8F10.0)
```

TABLE A-II

RHQ =	10.000 METERS		ZP =	0.000METERS	
TIME(SEC)	H	HI	HOA	HOI	HPHI
1.000E-07	5.017E+00	5.017E+00	7.91873799E+00	7.91873799E+00	1.58374760E+01
2.000E-07	1.186E+01	1.186E+01	2.36826061E+01	2.36826061E+01	4.73652123E+01
3.000E-07	1.841E+01	1.841E+01	3.76761115E+01	3.76761115E+01	7.53522229E+01
4.000E-07	2.486E+01	2.486E+01	4.85623400E+01	4.85623400E+01	9.71246800E+01
5.000E-07	3.125E+01	3.125E+01	5.66766303E+01	5.66766303E+01	1.13353261E+02
6.000E-07	3.762E+01	3.762E+01	6.26105857E+01	6.26105857E+01	1.25221171E+02
7.000E-07	4.397E+01	4.397E+01	6.69033441E+01	6.69033441E+01	1.33806688E+02
8.000E-07	5.032E+01	5.032E+01	6.99850044E+01	6.99850044E+01	1.39970009E+02
9.000E-07	5.666E+01	5.666E+01	7.21821334E+01	7.21821334E+01	1.44364267E+02
1.000E-06	6.299E+01	6.299E+01	7.37369889E+01	7.37369869E+01	1.47473978E+02
1.100E-06	6.932E+01	6.932E+01	7.48270517E+01	7.48270517E+01	1.49654103E+02
1.200E-06	7.565E+01	7.565E+01	7.55813996E+01	7.55813996E+01	1.51162799E+02
1.300E-06	8.198E+01	8.198E+01	7.60934888E+01	7.60934888E+01	1.52186978E+02
1.400E-06	8.830E+01	8.830E+01	7.64307961E+01	7.64307961E+01	1.52861592E+02
1.500E-06	9.463E+01	9.463E+01	7.66419591E+01	7.66419591E+01	1.53283918E+02
1.600E-06	1.009E+02	1.009E+02	7.67620042E+01	7.67620042E+01	1.53524008E+02
1.700E-06	1.073E+02	1.073E+02	7.68161473E+01	7.68161473E+01	1.53632295E+02
1.800E-06	1.136E+02	1.136E+02	7.68225446E+01	7.68225446E+01	1.53645089E+02
1.900E-06	1.199E+02	1.199E+02	7.67942763E+01	7.67942763E+01	1.53588553E+02
2.000E-06	1.262E+02	1.262E+02	7.67407751E+01	7.67407751E+01	1.53481550E+02
2.100E-06	1.326E+02	1.326E+02	7.66688522E+01	7.66688522E+01	1.53337704E+02
2.200E-06	1.389E+02	1.389E+02	7.65834347E+01	7.65834347E+01	1.53166869E+02
2.300E-06	1.452E+02	1.452E+02	7.64880942E+01	7.64880942E+01	1.52976188E+02
2.400E-06	1.515E+02	1.515E+02	7.63854269E+01	7.63854269E+01	1.52770854E+02
2.500E-06	1.578E+02	1.578E+02	7.62773254E+01	7.62773254E+01	1.52554651E+02
2.600E-06	1.641E+02	1.641E+02	7.61651748E+01	7.61651748E+01	1.52330350E+02
2.700E-06	1.705E+02	1.705E+02	7.60499927E+01	7.60499927E+01	1.52099985E+02
2.800E-06	1.768E+02	1.768E+02	7.59325309E+01	7.59325309E+01	1.51865062E+02
2.900E-06	1.831E+02	1.831E+02	7.58133472E+01	7.58133472E+01	1.51626694E+02
3.000E-06	1.894E+02	1.894E+02	7.56928586E+01	7.56928586E+01	1.51385717E+02
3.100E-06	1.957E+02	1.957E+02	7.55713789E+01	7.55713789E+01	1.51142758E+02
3.200E-06	2.021E+02	2.021E+02	7.54491459E+01	7.54491459E+01	1.50898292E+02
3.300E-06	2.084E+02	2.084E+02	7.53263414E+01	7.53263414E+01	1.50652683E+02
3.400E-06	2.147E+02	2.147E+02	7.52031057E+01	7.52031057E+01	1.50406211E+02
3.500E-06	2.210E+02	2.210E+02	7.50795481E+01	7.50795481E+01	1.50159096E+02
3.600E-06	2.273E+02	2.273E+02	7.49557545E+01	7.49557545E+01	1.49911509E+02
3.700E-06	2.336E+02	2.336E+02	7.48317931E+01	7.48317931E+01	1.49663586E+02
3.800E-06	2.400E+02	2.400E+02	7.47077189E+01	7.47077189E+01	1.49415438E+02
3.900E-06	2.463E+02	2.463E+02	7.45835762E+01	7.45835762E+01	1.49167152E+02
4.000E-06	2.526E+02	2.526E+02	7.44594015E+01	7.44594015E+01	1.48918803E+02
4.100E-06	2.589E+02	2.589E+02	7.43352249E+01	7.43352249E+01	1.48670450E+02
4.200E-06	2.652E+02	2.652E+02	7.42110716E+01	7.42110716E+01	1.48422143E+02
4.300E-06	2.715E+02	2.715E+02	7.40869628E+01	7.40869628E+01	1.48173926E+02
4.400E-06	2.779E+02	2.779E+02	7.39629165E+01	7.39629165E+01	1.47925833E+02
4.500E-06	2.842E+02	2.842E+02	7.38389480E+01	7.38389480E+01	1.47677896E+02
4.600E-06	2.905E+02	2.905E+02	7.37150706E+01	7.37150706E+01	1.47430141E+02
4.700E-06	2.968E+02	2.968E+02	7.35912957E+01	7.35912957E+01	1.47182591E+02
4.800E-06	3.031E+02	3.031E+02	7.34676334E+01	7.34676334E+01	1.46935267E+02
4.900E-06	3.094E+02	3.094E+02	7.33440923E+01	7.33440923E+01	1.46688185E+02
5.000E-06	3.158E+02	3.158E+02	7.32206802E+01	7.32206802E+01	1.46441360E+02
5.200E-06	3.284E+02	3.284E+02	7.29742692E+01	7.29742692E+01	1.45948538E+02
5.400E-06	3.410E+02	3.410E+02	7.27284457E+01	7.27284457E+01	1.45456891E+02
5.600E-06	3.537E+02	3.537E+02	7.24832457E+01	7.24832457E+01	1.44966491E+02
5.800E-06	3.663E+02	3.663E+02	7.22386980E+01	7.22386980E+01	1.44477396E+02
6.000E-06	3.789E+02	3.789E+02	7.19948258E+01	7.19948258E+01	1.43989652E+02
6.200E-06	3.916E+02	3.916E+02	7.17516477E+01	7.17516477E+01	1.43503295E+02
6.400E-06	4.042E+02	4.042E+02	7.15091788E+01	7.15091788E+01	1.43018358E+02
6.600E-06	4.168E+02	4.168E+02	7.12674315E+01	7.12674315E+01	1.42534863E+02
6.800E-06	4.294E+02	4.294E+02	7.10264158E+01	7.10264158E+01	1.42052832E+02
7.000E-06	4.421E+02	4.421E+02	7.07861398E+01	7.07861398E+01	1.41572280E+02

31

associated with the next set of parameters are initiated. Again, the values of the geometrical parameters together with the dummy constants precede the generated data.

After all computations indicated by the data cards have been completed, an end-of-file mark is written. Then a single entry consisting of four dummy constants having the value 2.2222E+22 is made followed by a final end-of-file mark. The purpose of this entry is to facilitate FORTRAN file manipulations in some of the auto editing and plot routines developed as an adjunct to this program.

DISTRIBUTION:

Dr. M. A. Uman
   Dept. of Electrical Engineering
   Univ. of Florida, Gainsville, Florida 32611

Dr. E. P. Krider
   Institute of Atmospheric Physics, Univ. of Arizona
   Tucson, Arizona 85721

Dr. D. K. McLain
   Westinghouse Research Laboratories
   Pittsburgh, PA 15235

Dr. Marx Brook
Prof. C. B. Moore
   New Mexico Institute of Mining and Technology
   Socorro, NM 87801

Dr. A. A. Few
   Space Science Dept., Rice University
   Houston, Texas 77001

Dr. H. Dolezalek
   Code 462
   Office of Naval Research
   Arlington, VA 22217

Dr. E. T. Pierce
   Stanford Research Institute
   Menlo Park, CA 94025

Dr. Carl Baum
Air Force Weapons Laboratory
Kirtland AFB, West
Albuquerque, NM 87115

1132	A. B. Church	5223	C. N. Vittitoe
1132	J. P. Luette	5600	A. Y. Pope
1150	J. R. Banister	8000	T. B. Cook, Jr.
1230	W. L. Stevens	8167	W. F. Gordon
1245	A. D. Thornbrough	8300	B. F. Murphey
1510	J. A. Hood	8322	R. Y. Lee
1560	E. E. Ives	8366	K. A. Mitchell
1562	W. R. Reynolds	9300	L. A. Hopkins, Jr.
1562	C. E. Jackson	9334	J. L. Mortley
1710	V. E. Blake, Jr.	9350	F. W. Neilson
1711	M. R. Madsen	9353	R. L. Parker
1730	H. H. Patterson	9353	R. D. Jones (3)
1731	J. E. Hinde	9540	L. M. Jercinovic
2110	E. G. Franzak	8266	E. A. Aas (2)
2120	G. W. Rodgers	3141	L. S. Ostrander (5)
2131	J. A. Cooper	3151	W. L. Garner (3)
2440	O. M. Stuetzer		For: ERDA/TIC (Unlimited Release)
2600	L. E. Hollingsworth		
2640	J. L. Tischhauser		ERDA/TIC (25)
2642	R. J. Detry		Attn: R. P. Campbell 3171-1
2642	H. A. Watts (3)		
5223	J. H. Renken		
5223	C. J. MacCallum		